EVS27 Symposium
Barcelona, Spain, November 17-20, 2013

Thermal modelling of large-format laminated Li-ion battery and experimental validation using embedded thermocouples

Bin Wu[1], Zhe Li[1], Jianbo Zhang[1*], Jun Huang[1]

Zhihua Nie[2], Ying Sun[2], Fuqiang An[2], Ningning Wu[2]

[1]*State Key Laboratory of Automotive Safety and Energy, Tsinghua University, Beijing 100084, China*

** Corresponding author, Correspond to jbzhang@mail.tsinghua.edu.cn*

[2]*CITIC Guoan MGL Power Technology CO.,LTD, Beijing 102200, China*

Abstract

Thermal modelling for lithium ion batteries is important to evaluate battery thermal safety and to refine battery thermal designs. To develop a reliable and efficient thermal model, the following key factors needs to be addressed: the techniques to accurately determine the thermal parameters and heat generation rates, the reasonably simplified thermo-electrical equations and the experimental validation. In this study, a new transient method is developed to measure the thermal parameters of a large-format laminated battery. The reversible and irreversible heat generation rates were measured for different states of charge and temperatures. With the measured thermal parameters and heat generation rates, the temperature distribution of the battery was predicted based on a thermal-electrical coupled model. The prediction was found in good agreement with embedded-sensor experimental results.

Keywords: Thermal modelling, Thermal parameter, Embedded-thermocouples, Lithium-ion battery

1 Introduction

Due to its high energy density and long cycle life, Li-ion battery is the most widely used power sources for the electric vehicles. Compared with the Li-ion battery used in the commercial electrical product like the mobile phone, laptop, etc., the Li-ion battery for traction use usually have much larger capacity. This increase in capacity and size easily leads to the development of temperature variation inside the battery. Under severe conditions, local hot spots may emerge, impairing durability and even triggering safety problems. Simulation based on thermal models is an important method to elucidate the processes underlying the temperature distributions, to evaluate battery thermal safety, and to refine battery thermal designs.

Thermal modeling for different kinds of batteries is of great interest in the literature. The basic thermal equilibrium model is:

$$\rho C_{\mathrm{p}} \frac{\partial T}{\partial t} = \nabla \cdot (k \nabla T) + q \qquad (1)$$

Where ρ is the density, C_{p} is the heat capacity, T is the temperature, k is the thermal conductivity and q is the heat generation rate of the battery.

1.1 Thermal parameters

Original thermal parameter measurement reports for lithium ion batteries were not easily found in the literature. Many researchers simply report the thermal parameters without describing measurement methods. Fleckenstein et al. have shown that the nearly one-order magnitude discrepancy of thermal parameters would lead to a difference of one-order magnitude for the predicted temperature gradient [1]. Thus, the original methods to measure the thermal parameters should be further explored to achieve better prediction of battery thermal behaviour.

The heat capacity is generally determined by measuring the relationship between the temperature change and absorbed/dissipated energy of the sample in a calorimeter. Maleki et al. measured the heat capacity of an 18650 battery using a transient cooling method in an adiabatic calorimeter. Pesaran et al. measured the heat exchange between a cell and a calorimeter using heat flux sensors and the temperature difference to determine the heat capacity.

The battery thermal conductivities can be measured by both steady and transient methods. Maleki et al. measured the parallel (in-plane) and perpendicular (through-plane) thermal conductivities of a three-layer stack, including a piece of negative electrode, positive electrode and separator using hot plate technique (HPT) and xenon flash technology (XFT).

1.2 Heat generation rates

Heat generation inside batteries is a complex process that requires a detailed electrochemical model. The most commonly used model was simplified from Bernardi model [2], as shown in Eq. (2).

$$q = I(U - V) - IT\frac{\partial U}{\partial T} \quad (2)$$

The first term is the irreversible heat including the ohmic losses, charge transfer over-potential and mass transfer limitations. The second term is the entropic heat. Phase change and mixing heat terms are neglected in the model. Various measurement methods and modeling methods are derived to define the heat source term in thermal models.

1.2.1 Measurement methods

Various measurement methods were developed to obtain accurate and reliable heat generation data.

The irreversible heat is a summation of activation, concentration and ohmic losses. Over-potential resistance is used to quantify the over-potential for different currents. Onda et al. presented four different methods to measure the over-potential resistance, including measuring the voltage-current characteristics of batteries during the constant-current discharge, the difference between the open-circuit voltage and the cell voltage, the voltage change during the intermittent discharge for 60 s, and the ac impedance [3].

The reversible heat rate is commonly determined by measuring the open circuit potential (OCP) variation with temperature at a fixed state of charge (SOC). Long waiting time for the steady OCP and the self-discharge during the waiting time are two main drawbacks for this method. Another measurement method is based on the assumption that the entropy heat rate remains constant in discharge and charge processes. Thus, the reversible heat rate is calculated by subtracting the charge calorimeter data from discharge.

1.2.2 Modelling methods

Heat generation inside the battery is defined as a source term of the thermal equation. The source term was usually coupled with a simplified electrical model or an electrochemical model.

Kim et al. presented an electric-thermal coupled model to study the thermal and electrical behaviour, optimize electrode configuration and investigate combined effects of the electrical and thermal contact resistances between current collecting tabs and lead wires [4-8]. The heat source term was defined as

$$q = aJ(E_{oc} - E - T\frac{dE_{oc}}{dT}) + a_p r_p i_p^2 + a_n r_n i_n^2 \quad (3)$$

where a, a_p, a_n are the specific areas, J is the transferred current density, E_{oc} is the open circuit voltage, E is the cell voltage, r_p and r_n are the resistance of electrodes, i_p and i_n are the planar current density. The current densities were calculated from a two-dimensional electrical model.

The pseudo two-dimensional electrochemical model (P2D) presented by Doyle was frequently

referred to account for the electrochemical behavior in a electrochemical-thermal model [9-13]. The heat source term from the P2D model was

$$q = \sum_j a_{sj} i_{nj} (\phi_s - \phi_e - U_j) + \sum_j a_{sj} i_{nj} T \frac{\partial U_j}{\partial T} \quad (4)$$
$$+ \sigma^{eff} \nabla \phi_s \cdot \nabla \phi_s + \kappa^{eff} \nabla \phi_e \cdot \nabla \phi_e + \kappa_D^{eff} \nabla \ln c_e \cdot \nabla \phi_e$$

The coupled electrochemical-thermal model was used to study the temperature, current, potential and chemistry concentration distribution for large format lithium ion batteries.

1.3 Experimental validation

The predicted temperatures are validated by experimental results to confirm the accuracy of thermal models. Existing reports usually measure the surface temperature by thermocouples or infrared thermography. Hallaj et al. compared the simulation results with measurement results from a single thermocouple on an 18650 battery [14]. Kim et al. measured the temperature distribution using infrared thermography to validate the predicted temperatures [8]. However, direct internal temperature validation is rarely found in the literature due to the difficulty of inner temperature measurement methods. Thermal models are developed to study the temperature distribution of the whole battery, especially for the positions where measurement is difficult or impossible. The lack of direct inner temperature validation makes the prediction results questionable.

In addition, the existing studies usually validate the simulation results for different operation conditions but only for one boundary condition. Boundary conditions significantly influence the temperature distribution and evolution during operations. Thus, the validation experiment validation should be conducted for different boundary conditions to improve the sufficiency.

In summary, to develop a reliable and efficient simulation model, the following key factors needs to be addressed: the techniques to accurately determine the thermal parameters, the model of heat generation rates, the reasonably simplified thermo-electrochemical equations and the experimental validation with both internal and external information.

In this study, we are trying to develop a thermal model for a large-format laminated Li-ion battery and validate it using information measured with embedded thermo-couples [15].

2 Determination of thermal parameters

Large-format lithium-ion batteries usually have laminated structure and Al-plastic film packages. These characteristics require specific method to measure the thermal parameters:

(1) The battery core consists of many electrode and separator layers, thus the difference between the layers can be ignored and the core can be simplified as the homogeneous composite. The core equivalent thermal parameters are defined to depict the overall thermal properties.

(2) The core with layered structure has isotropic thermal conductivities in perpendicular and parallel directions. The isotropic thermal conductivities should be measured simultaneously while the HPT method can only deal with one direction.

(3) The thermal property of the Al-plastic film significantly differs from the core. Besides, there exists thermal resistance between the film and the core. Therefore, the Al-plastic film should be considered separately in the measurement. The ‘serial and parallel’ calculation based on individual composition properties is not well suited due to the unknown resistance.

(4) The presence of electrolyte significantly affects the battery thermal properties, and the thermal parameters should be measured in-situ to prevent electrolyte leakage and ensure the measurement results representative of real battery property. XFT is not applicable because the method requires specially prepared samples.

In summary, an in-situ measurement method should be developed to simultaneously obtain heat capacity, isotropic thermal conductivities and thermal resistance between the film and the core for laminated batteries.

A new method is proposed in this study to measure the effective specific heat capacity and the thermal conductivities of the laminated battery. A planar heat source was attached to the center of one surface, and the transient temperature distribution on the opposite surface was recorded. The temperature distribution in the tested

structure was modelled using a finite element model. In this model, the necessary thermal parameters were initialized with the values from literature. By comparing the measured and simulated results, the accuracy of the thermal parameters was quantified by a weighted root-sum-square error criterion. Parameters were estimated by minimizing the error criterion using the general multi-objective optimization software modeFRONTIER [3].

2.1 Experimental

Figure 1 is a schematic diagram of the experimental setup. A circular ceramic heater (25 mm diameter and 1 mm thick) was placed between two identical batteries. Heat-conducting silicone grease was used to ensure the close contact between the battery and the heater. The two batteries were covered from upside and downside by polyfoam with good thermal insulation. Four thermocouples were located at each interface of the battery and the polyfoam insulation. The experimental setup was sandwiched between two thin steel plates using four threaded rods to hold the layers firmly. The apparatus was placed in a furnace to minimize the heat loss from the battery surface.

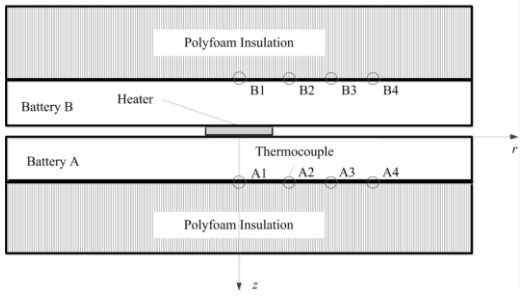

Figure 1: Schematic diagram of the experiment setup for thermal parameter measurement

2.2 Estimation Procedures

There are several assumptions to develop a simplified thermal model.

(1) The battery core was assumed to be homogeneous with equivalent thermal parameters.

(2) The heater diameter was small compared with the battery size, thus the boundary effect of heat conductivity was neglected. The temperature distribution of the battery core was assumed to be axially-symmetric during the experiment.

(3) The heat flux was assumed uniform over the heating area and equal between the two surfaces.

(4) The polyfoam insulation could provide adiabatic environment for the battery during the experiment.

The simplified 2D symmetrical model of the battery structure was shown in Figure 2.

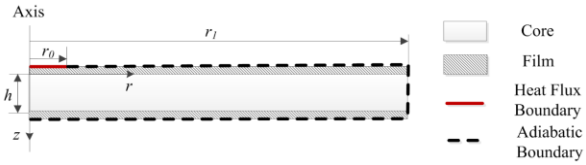

Figure 2: Schematic view of the finite element model

Due to the axial symmetry of the model, the plastic film and the core are respectively depicted by two dimensional sub-models in this figure.

The governing equation of heat transfer can be written as,

$$\rho C_p \frac{\partial T}{\partial t} = k_r \left(\frac{\partial^2 T}{\partial r^2} + \frac{1}{r}\frac{\partial T}{\partial r}\right) + k_z \frac{\partial^2 T}{\partial z^2} \quad (5)$$

Where ρ is the mass density in kg m^{-3}, C_p is the specific heat capacity in J kg^{-1} K^{-1}, k_r is the radial thermal conductivity in W m^{-1} K^{-1}, k_z is the axial thermal conductivity, and T is the temperature.

In the area where the heater was placed, the boundary heat flux was defined as,

$$q = \frac{q(t)}{2}, z = 0, 0 \le r \le r_0; \quad (6)$$

Where $q(t)$ is the transient power delivered by the heater.

The heat flux between the film and the core was assumed to be proportional to the temperature difference,

$$q_n(r,z) = \lambda(T_{\text{Core}}(r,z) - T_{\text{Film}}(r,z)) \quad (7)$$

Where: λ is the thermal conductance between the core and the film.

All outer boundaries except for the heater-battery interface are assumed adiabatic as indicated in Figure 2.

In the optimization procedure, the film thermal parameters were estimated from known material properties. The core specific heat capacity and thermal conductivities as well as the thermal

conductance were considered as variables and needed to be estimated from the experimental data.

The basic process to estimate the parameters is to minimize a weighted root-sum-square error criterion S between the measured and the calculated temperatures,

$$S = (Y - \hat{T})^T W (Y - \hat{T}) \tag{8}$$

Where Y is the calculated temperature, T is the measured temperature and W is the weight matrix.

The accuracy of the thermal parameters was quantified by the criterion. The thermal parameters were finally obtained at the moment that the criterion reached the minimum.

These procedures were implemented with two commercial software packages, COMSOL and modeFrontier. COMSOL was used to simulate the temperature distribution and evolution with the inputs of different thermal parameters. ModeFrontier was used to minimize the criterion using optimization algorithms.

2.3 Results

Using the analysis procedures described in section 2.2, the thermal parameters of this cell could be optimized via modeFrontier. The results are listed in Table 1.

Table 1 Optimization results

Parameter	Optimization range	Optimization Results
k_r ($W \cdot m^{-1} \cdot K^{-1}$)	0~40	21
k_z ($W \cdot m^{-1} \cdot K^{-1}$)	0~5.0	0.48
C_p ($J \cdot kg^{-1} \cdot K^{-1}$)	700~3000	1243
λ ($W \cdot m^{-2} \cdot K^{-1}$)	100~2000	1300

The experimental and computational temperature results are compared in Figure 3.

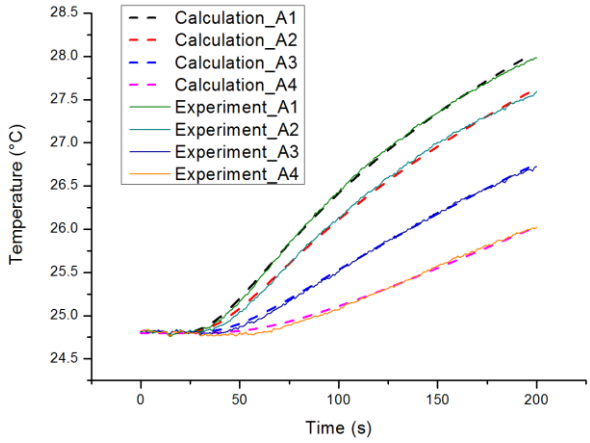

Figure 3: Comparison of computational and experimental results

The battery heat capacity was also measured by an accelerating rate calorimeter (ARC) and a heat-flow calorimeter (HFC). The ARC result was 1.05~1.19 $Jg^{-1}K^{-1}$ at the temperature range between 30~50 °C and the HFC result was 1.03 ± 0.14 $Jg^{-1}K^{-1}$ at 25 °C. Both results show good agreement with the value listed in Table 1.

3 Measurement of heat generation rates

Heat generation inside batteries was divided into reversible and irreversible parts in Bernardi heat generation model [2]. In this study, the reversible heat generation rates were estimated by entropy coefficients while the irreversible parts were quantified by over-potential resistances. Different methods were used to measure the two heat source terms. The total heat generation rates were measured in an adiabatic calorimeter to validate the separate measurement results.

3.1 Reversible heat

The reversible heat is attributed to the entropy change of the lithium insertion/extraction reactions. The rates of reversible heat generation are defined as,

$$Q_{rev} = -IT \frac{\partial E}{\partial T} \tag{9}$$

where $\partial E / \partial T$ is the derivatives of open circuit voltages (OCV) with respect to temperatures.

The OCVs were measured for 10 ℃, 15 ℃, 20 ℃, 25 ℃, 30 ℃ and 35 ℃ at a fixed state of charge (SOC) as shown in Figure 4. The slopes of the

fitted linear OCV-Temperature curves were calculated as the entropy coefficients.

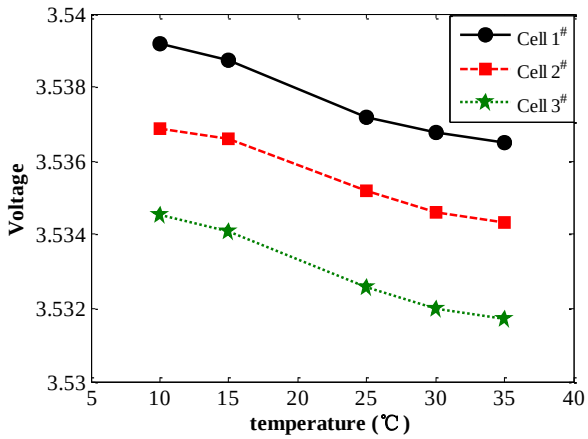

Figure 4: The open circuit voltages for different temperatures at SOC=10%

The entropy coefficients for different SOC were measured as shown in Figure 5.

Three individual cells were used in the experiments. The results in Figure 5 show good agreement among the three cells.

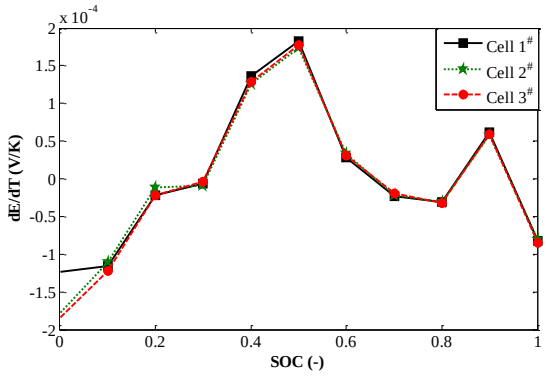

Figure 5: Entropy coefficients for different SOC

3.2 Irreversible heat

Various methods were developed to measure the over-potential resistance, including V-I characteristics, intermittent discharge/charge and ac impedance.

V-I characteristics were obtained from constant current charge/discharge tests at different current rates and temperatures. The charge/discharge curves were converted to the voltage–current (V–I) characteristics as parameters of SOC and temperature. The over-potential resistance was then given by the slopes of the V-I characteristics for various temperatures and SOC.

However, significant temperature rise was recorded during charge/discharge for large-format batteries even at low current rates, thus the constant temperature assumption was no longer valid for large-format batteries. This study presented an alternative method using a small model cell to eliminate the temperature rise. The model cell consisted of only two pairs of active electrodes with same chemistry composition. The capacity of the model cell was 270 mAh and the dimensions were 8 cm × 10 cm. Discharge test results showed that the temperature rise of the model cell was within 1 ℃ for 2C current rates. The over-potential resistance for large-format batteries was calculated by

$$R_{\mathrm{L}} A_{\mathrm{L}} N_{\mathrm{L}} = R_{\mathrm{m}} A_{\mathrm{m}} N_{\mathrm{m}} \qquad (10)$$

Where R is the over-potential, A is the active electrode area, N is the number of active electrode pairs, L refers to large-format batteries and m refers to model cells.

The equivalence between model cells and large-format batteries was validated by comparing their area-specific electrochemical impedance spectrum.

The measurement over-potential resistance by V-I characteristics at different SOC and temperatures is shown in Figure 6.

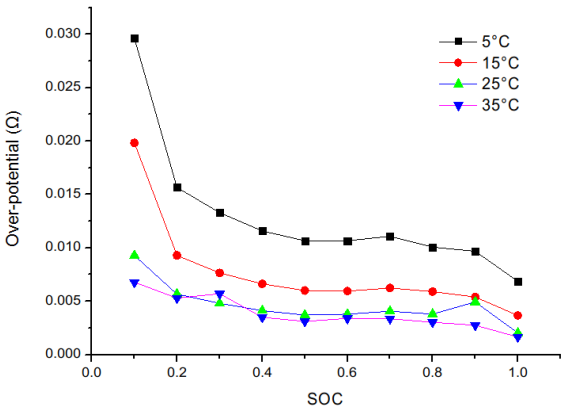

Figure 6: Over-potential resistance for different SOC and temperatures

Measurement results from intermittent charge/discharge and energy loss method showed good agreement with results in Figure 6.

3.3 ARC measurement

Accelerating rate calorimeter is a kind of adiabatic calorimeter. ARC can provide quasi-adiabatic environment for the sample by diminishing the temperature difference between the sample and the chamber using sensors and

heaters. The heat generated by the sample is quantified by the temperature increase of the sample with known heat capacity.

A 25 Ah battery was discharged at 1C rate in the ARC chamber. 12 thermocouples were attached on the battery surface to detect the temperature evolution. The heat generation rates were calculated by the average temperature increase rates. The measurement results were revised using a first-order inertia model to eliminate the time lag due to thermal conduction inside the battery.

The results in Figure 7 shows that the calculated temperature increase rates from indirect methods achieve good agreement with direct measurement results by ARC. Thus, the experiment validated the measurement results in section 3.1 and 3.2.

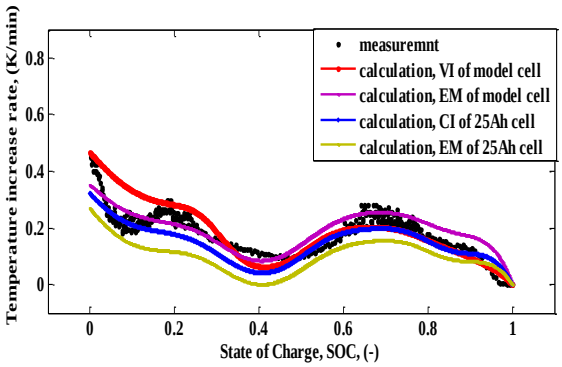

Figure 7: ARC measurement result compared with indirect methods

4 Model development

A thermal-electrical coupled model was developed to predict battery temperature distribution for different operating and boundary conditions. The detailed layer structure of the battery core is ignored to simplify the model. Although neglecting the structural details, the model considered the anisotropic thermal conductivities. The core is assumed to be an assembly of infinitely identical micro batteries. Those micro batteries are electrically connect in parallel [16].

In the thermal model, the temperature distribution was calculated by the energy balance equation,

$$\rho C_p \frac{\partial T}{\partial t} = k_x \frac{\partial^2 T}{\partial x^2} + k_y \frac{\partial^2 T}{\partial y^2} + k_z \frac{\partial^2 T}{\partial z^2} + q \quad (11)$$

where ρC_p is the volume heat capacity, k_x, k_y, k_z are the thermal conductivities, q is the heat generation rate.

The heat generation rate can be expressed as,

$$q = i^2 r - iT \frac{\partial E}{\partial T} \quad (12)$$

where r is the over-potential resistance and $\frac{\partial E}{\partial T}$ is the entropy coefficient.

The over-potential resistance depends on SOC and temperature while entropy coefficients vary only with SOC. The relationships are determined from measurement results in section 3,

$$r = f(\mathrm{SOC}, T), \frac{\partial E}{\partial T} = g(\mathrm{SOC}) \quad (13)$$

Heat generation rates in tab areas are calculated using tab material resistance,

$$q_+ = i^2 r_{\mathrm{Al}}, q_- = i^2 r_{\mathrm{Cu}} \quad (14)$$

In the electrical model, the current density and SOC were assumed non-uniform, the definition of local SOC in micro batteries is

$$\frac{ds}{dt} = -\frac{i}{c_i} \quad (15)$$

where s is the local SOC, i is the current density, c_i is the local capacity.

The micro batteries are assumed to be connected in parallel, thus each micro battery shares the same terminal voltage,

$$i = \frac{E_0 - E}{r_i} \quad (16)$$

where E_0 is the OCV, E is the terminal voltage, r_i is the local over-potential resistance.

The discharge current is the integration of the current density over the core,

$$I = 4 \iiint_V i \mathrm{d}x\mathrm{d}y\mathrm{d}z \quad (17)$$

where I is the applied current.

The boundary conditions are defined as

$$q_f = h(T - T_0) \quad (18)$$

where h is the convection coefficient and T_0 is the environmental temperature.

The initial conditions are defined as

$$\mathrm{SOC} = 1.0, T = T_0 \qquad (19)$$

5 Experimental Validation

The accuracy of the coupled thermo-electrochemical battery model as well as the thermal parameters and the heat generation rates needs to be validated with experiment. An adequate validation requests information measured both on the surface of and inside the battery. However, in most of the previous validation, only the surface temperature, usually at one location was used to validate the models. The scarcity of internal information hinders the accuracy of the model validation, leaving its predicting capability questionable.

In this study, an embedded-sensor method was developed to measure the temperature at multiple locations inside the battery. The embedded-sensor positions (A1~A12) are shown in Fig.3.

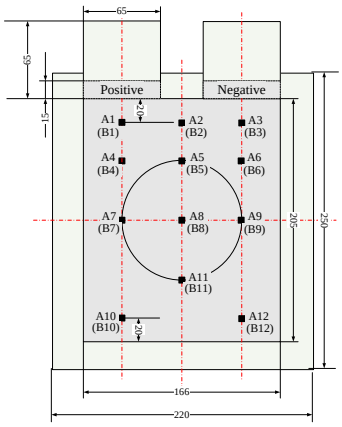

Figure 8: Embedded-sensor locations

The validation experiments were conducted for different discharge rates and different boundary conditions, including natural convection, forced convection and adiabatic. The simulated temperature distributions were in good agreement with the experimental results.

Figure 9 shows the experimental and simulation temperatures of A1 and A4 for 1C discharge in adiabatic environment.

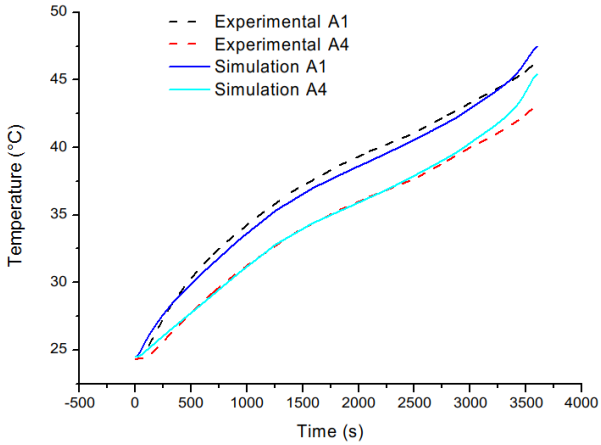

Figure 9 Temperatures of A1 and A4 for 1C discharge in adiabatic environment

6 Conclusion

A new transient method combined with finite-element-based modelling and optimization for determining the thermal parameters of large-format laminated Li-ion battery was developed. The heat generation rate of the battery was measured under different temperature and SOC.

The measured thermal parameters and the calculated heat generation rate were incorporated into a thermal-electrochemical coupled model to predict the temperature distribution of battery under different operating and boundary conditions.

The model was validated by comparison with the experimental data from multiple embedded thermocouples. There was a good agreement between the simulation and experiment results. The direct measurement of internal temperature with embedded sensors can also provide useful information for improving battery thermal design.

Acknowledgments

This work is supported by the National Natural Science Foundation of China under the grant number of 51207080, the Independent Research Programs of Tsinghua University under the subject number of 2011Z01004, and the China Postdoctoral Science Foundation under the grant number of 2012M510436.

References

[1] M. Fleckenstein, S. Fischer, O. Bohlen, and B. Baker, "Thermal impedance spectroscopy - a method for the thermal characterization of high power battery cells," J Power Sources, vol. 223, pp. 259-267, 2013.

[2] D. BERNARDI, E. PAWLIKOWSKI and J. NEWMAN, "A general energy-balance for battery systems b-8650-2008," J Electrochem Soc, vol. 132, pp. 5-12, 1985.

[3] K. Onda, H. Kameyama, T. Hanamoto, and K. Ito, "Experimental study on heat generation behavior of small lithium-ion secondary batteries," J Electrochem Soc, vol. 150, pp. A285-A291, 2003.

[4] J. Yi, U. S. Kim, C. B. Shin, T. Han, and S. Park, "Three-dimensional thermal modeling of a lithium-ion battery considering the combined effects of the electrical and thermal contact resistances between current collecting tab and lead wire," J Electrochem Soc, vol. 160, pp. A437-A443, 2013.

[5] U. S. Kim, J. Yi, C. B. Shin, T. Han, and S. Park, "Modelling the thermal behaviour of a lithium-ion battery during charge," J Power Sources, vol. 196, pp. 5115-5121, 2011.

[6] U. S. Kim, J. Yi, C. B. Shin, T. Han, and S. Park, "Modeling the dependence of the discharge behavior of a lithium-ion battery on the environmental temperature," J Electrochem Soc, vol. 158, pp. A611-A618, 2011.

[7] U. S. Kim, C. B. Shin and C. S. Kim, "Modeling for the scale-up of a lithium-ion polymer battery," J Power Sources, vol. 189, pp. 841-846, 2009.

[8] U. S. Kim, C. B. Shin and C. S. Kim, "Effect of electrode configuration on the thermal behavior of a lithium-polymer battery," J Power Sources, vol. 180, pp. 909-916, 2008.

[9] M. Guo and R. E. White, "A distributed thermal model for a li-ion electrode plate pair," J Power Sources, vol. 221, pp. 334-344, 2013.

[10] K. Lee, K. Smith, A. Pesaran, and G. Kim, "Three dimensional thermal-, electrical-, and electrochemical-coupled model for cylindrical wound large format lithium-ion batteries," J Power Sources, vol. 241, pp. 20-32, 2013-11-01 2013.

[11] L. Cai and R. E. White, "Mathematical modeling of a lithium ion battery with thermal effects in comsol inc. Multiphysics (mp) software," J Power Sources, vol. 196, pp. 5985-5989, 2011.

[12] V. Srinivasan and C. Y. Wang, "Analysis of electrochemical and thermal behavior of li-ion cells," J Electrochem Soc, vol. 150, pp. A98-A106, 2003.

[13] G. H. Kim, K. Smith, K. J. Lee, S. Santhanagopalan, and A. Pesaran, "Multi-domain modeling of lithium-ion batteries encompassing multi-physics in varied length scales," J Electrochem Soc, vol. 158, pp. A955-A969, 2011.

[14] S. Al Hallaj, H. Maleki, J. S. Hong, and J. R. Selman, "Thermal modeling and design considerations of lithium-ion batteries," J Power Sources, vol. 83, pp. 1-8, 1999.

[15] Z. Li, J. Zhang, B. Wu, J. Huang, Z. Nie, Y. Sun, F. An, and N. Wu, "Examining temporal and spatial variations of internal temperature in large-format laminated battery with embedded thermocouples," J Power Sources, vol. 241, pp. 536-553, 2013-11-01 2013.

[16] Y. Inui, Y. Kobayashi, Y. Watanabe, Y. Watase, and Y. Kitamura, "Simulation of temperature distribution in cylindrical and prismatic lithium ion secondary batteries," Energ Convers Manage, vol. 48, pp. 2103-2109, 2007.

Authors

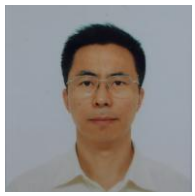

Jianbo Zhang

Ph.D., The University of Tokyo, Japan.

Professor, Tsinghua University, China.

Worked in the field of fuel cell and battery in Nissan Research Center for 11 years.

Current research interests include the thermal characteristics of large format lithium ion battery, thermal management of battery package, fast charging technique at low temperature.

Research on the PEM fuel cell, such as the mass transport inside the membrane-electrode-assembly, water management and durability, is also being undertaken.